

Iron technology in medieval Kerala: archaeometallurgical studies on iron artefacts from Triprangode

Mo Rizwan Ahmad Qureshi¹, Nishkarsh Srivastava¹, Alok Kumar Kanungo^{1,2,*}, Amit Arora¹ and Krishna Raj, K.³

¹Indian Institute of Technology, Palaj, Gandhinagar 382 055, India

²College of Humanities, Arts and Social Sciences, Flinders University, Adelaide 5001, Australia

³Pazhassiraja Archaeological Museum, East Hill, Kozhikode 673 005, India

Iron was a new entrant and a must in weaponry in the 2nd and 1st millennium BCE. There is every possibility of iron being used for generations, and deposited or hidden it for use in the times of need or even as a part of religious activities. Dating iron has been mostly based on the associated finds, and iron has been repeatedly melted, shaped and reused. Differentiating the iron in use at present from that in earlier times has been a challenge, and requires the dating of artefacts. Chemical objects characterization is contextual-specific. Three iron objects recovered from a cave near Triprangode, Kerala, India was studied using various analytical techniques to understand the metallurgical characteristics such as microstructure, phases, inclusions and production technology. The artefact was also dated using accelerator mass spectroscopy (AMS). The three artefacts included two swords and a tripod, which were reported to belong to the 1st millennium BCE based on associated pottery finds and typological comparison. Optical microscopy and scanning electron microscopy techniques were employed for microstructure analysis. X-ray fluorescence analysis was used to identify the elements present in the samples. X-ray diffraction and energy dispersive X-ray spectroscopy analyses were performed to identify the phases present in the samples. AMS radiocarbon dating was carried out to determine the age of the artefacts. A combination of these techniques helped identify the iron-making process.

Keywords: Archaeometallurgical studies, AMS dating, iron artefacts, medieval period, microstructure.

ANCIENT iron reveals the metallurgical and pyro-technology of the ancient people knowledge. Iron was mainly used to make tools for household and agricultural objects, and in armour. Wootz steel has been a subject of research, which is mainly found in the northern part of South India¹. There have been few studies on the antiquity and metallurgy of ancient iron recovered from the southern part of South India².

Studies suggest that iron came into use in North and South India before the mid-second millennium BCE³. From the 17th century, South Indian steel was imported by the Western world with the famous Damascus swords, mainly made of wootz steel. Records of this are found in the accounts of several travellers and archaeological finds.



Figure 1. Site of artefacts recovery located in the map of Kerala, India⁹.

*For correspondence. (e-mail: alok.kanungo@iitgn.ac.in)



Figure 2. The recovered potteries and iron artefacts.

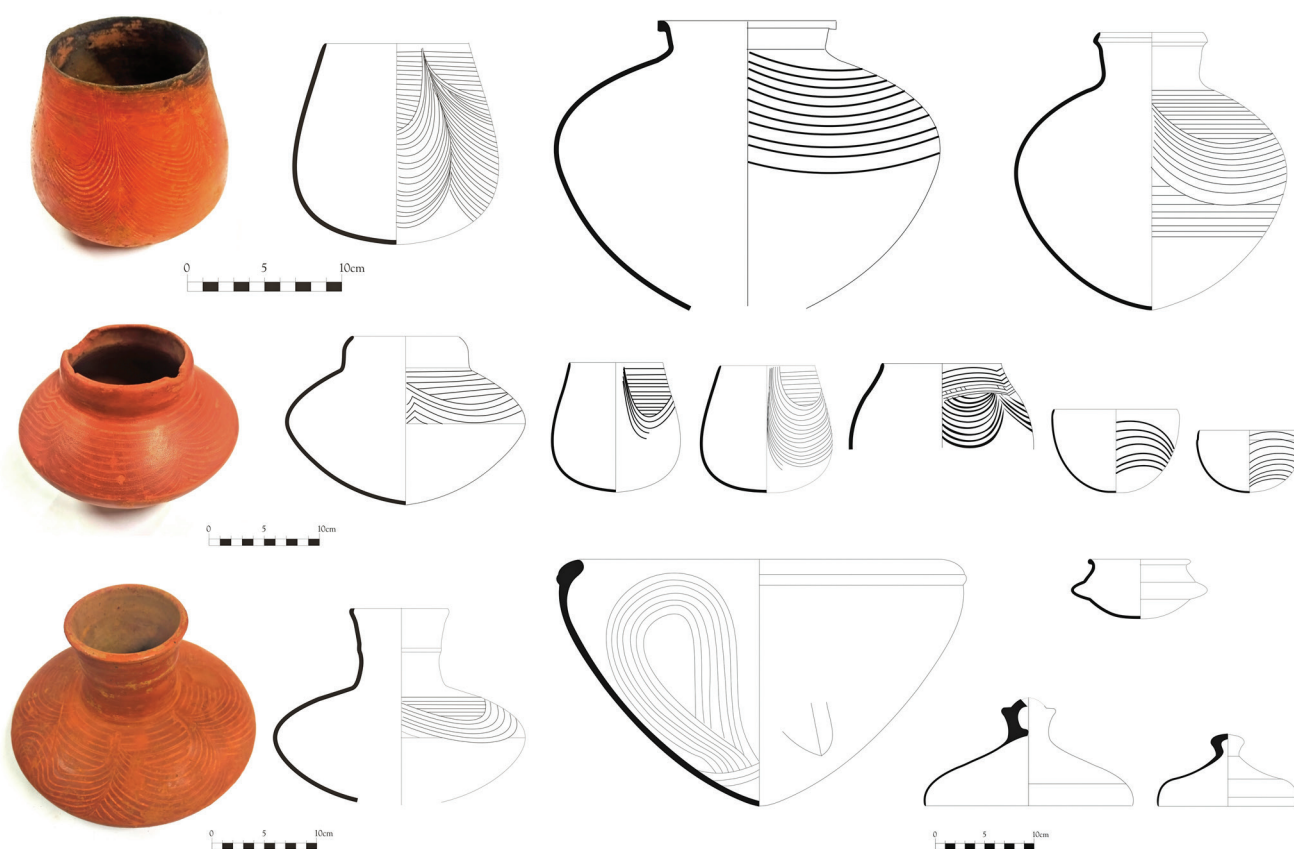


Figure 3. Pots and painted decorations.

Crucible iron and bloomery iron furnaces were the two primary iron production techniques in ancient times. The older bloomery iron furnace was used to make low-carbon steel³⁻⁶.

Site of recovery and artefacts

In 2020, two iron swords, one tripod and 16 potteries were found in a rock-cut cave (10°51'40"N lat. and 75°57'51"E long.) in Kodakkal, Malappuram district, Kerala, India during levelling work in the premises of a newly built house

(Figure 1)⁷. In Malayalam (the local language), Kodakkal means umbrella stone, a monument associated with the Iron Age in this region. Many such iron age monuments have been discovered in the region, including neighbouring Thirunavaya in Malappuram district^{7,8}. Based on the morphology of the iron artefacts in general, the tripod in particular and signature black and red ware, the assemblages were reported as belonging to of the early iron age (1st millennium BCE). The outside of most of the potteries had a fine slip of red coating; in some cases, the interior also had the same slip (Figure 2). Painted decorations found inside a conical



Figure 4. Identical design on a potsherd found at Porunthal and dish from Triprangode.

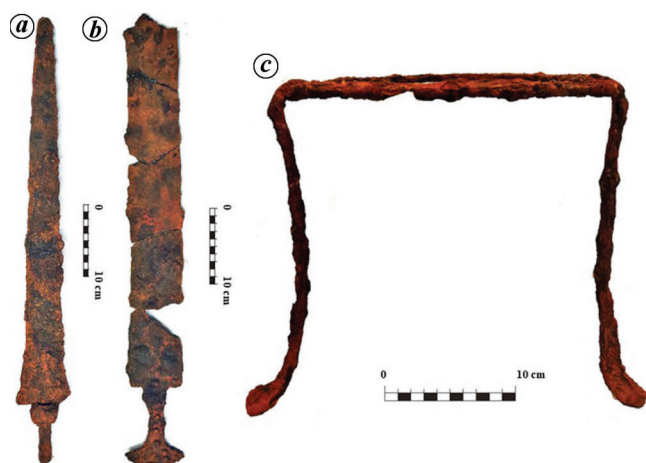


Figure 5. Iron objects: (a) pointed-tip sword, (b) broad-tip sword and (c) tripod.

Table 1. Specifications of the recovered iron objects

Sample name	Sample	Length (cm)	Width (cm)	Weight (g)
A (TPRGD-17)	Sword/dagger	61.5	8	868
B (TPRGD-18)	Sword	58	6.5–7	704
C (TPRGD-19)	Tripod stand	25	24 (diameter)	599

jar and a small dish have not been reported from any other site so far. Such painted decorations stand out among the 1st millennium BCE sites in Kerala. The paintings and patterns show similarities with the russet-coated painted ware recovered from Maniyur in Kozhikote district (displayed in Pazhassiraja Museum) and Attappadi in Palakkad district, Kerala (Figure 3) and with iron age pottery from Porunthal (77°28'38"N lat. and 10°21'28"E long.) an archaeological site in the Western Ghats of Tamil Nadu, India)¹⁰ (Figure 4).

Iron artefacts

The artefacts consisted of three iron objects, among two swords and a tripod stand (Figure 5). The objects were corroded and covered with a thick layer of rust. One pointed end tipped sword (TPRGD-17; sample a) was double-edged.

The blade was around 8 cm while at the place of the hilt. A ring was seen on the tang, probably the bolster of the wooden handle. The second sword (TPRGD-18; sample b) had a thin blade. It had broken into many pieces, and the tip and some parts of the blade were missing. The hilt consisted of a grip and pommel. Some rivets were seen on the hilt. These rivets may have been used for sandwiching iron tang between two halves of the wooden handle. The tripod (sample c; a leg was missing) is the most common type of object present in almost all the Iron Age Megalithic rock-cut chambers in South India. Table 1 shows the specifications of the recovered iron artefacts.

Materials and methods

Three individual broken pieces of artefacts were received for analysis. The cut samples were cleaned and rust was removed in order to obtain the core material for characterization. The following metallurgical and spectroscopic analyses were carried out:

(i) For elemental composition, X-ray fluorescence (XRF) analysis (Panalytical Epsilon1) was carried out using Ag-K α radiation in 'Omnian' scan mode.

(ii) For identifying the phases, X-ray diffraction (XRD) analysis (Bruker Discover D8) was carried out at 0.3 steps/sec with a scanning speed of 0.02°/sec in angle range of 20°–100°.

(iii) Small pieces of the respective samples were then sectioned using the 'Isomet' slow-speed diamond blade cutter for microstructural analysis. The cut portions were mounted in epoxy resin cold mountings for ease of polishing. After polishing on sets of emery paper, the samples are then polished on velvet cloth to eliminate all the fine scratches from the sample surface and obtain mirror finish. The polished samples were etched using Nital reagent (10% HNO₃ solution in ethanol) to reveal the microstructure after an ultrasonic bath in ethanol for 10 min.

(iv) The etched samples were observed under an optical microscope (OM) and a scanning electron microscope (SEM). The microstructures were observed under the OM (Zeiss) at different magnifications (100×–500×). The samples were also analysed using a field emission scanning electron microscope (FESEM; Jeol JSM-7600F).

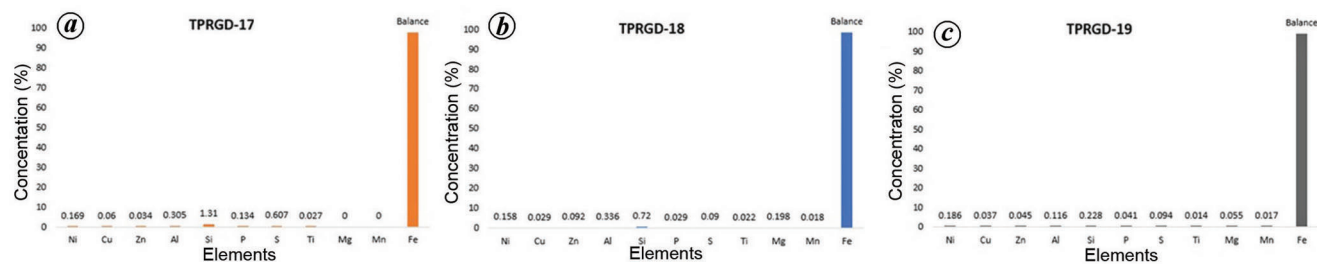


Figure 6. XRF analysis results of (a) sword (sample a), (b) sword (sample b) and (c) tripod (sample c).

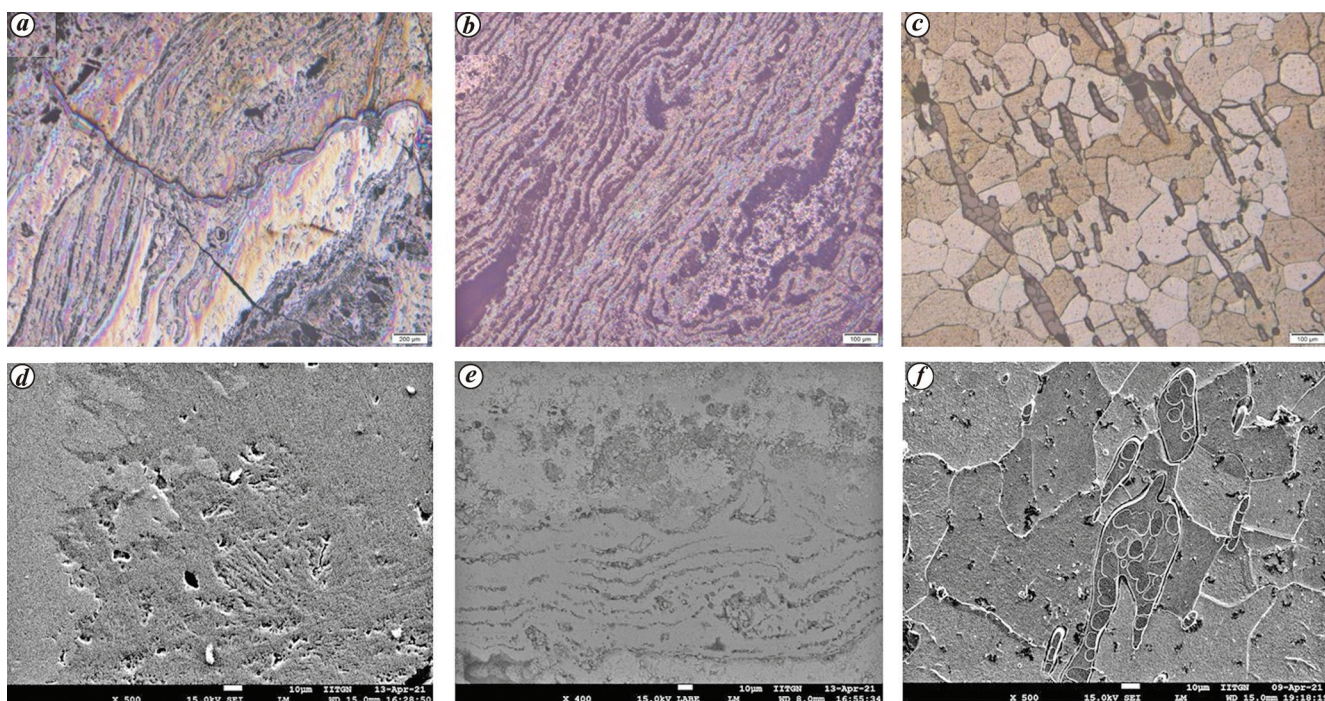


Figure 7. Optical microscope images of (a) sword (sample a), (b) sword (sample b) and (c) tripod (sample c). Scanning electron microscope images of (d) sword (sample a), (e) sword (sample b) and (f) tripod (sample c).

(v) Elemental analysis was carried out using energy dispersive X-ray spectroscopy (EDS; Oxford) embedded in FESEM to detect elements whose atomic numbers were more than 8.

(vi) Finally, accelerator mass spectrometry (AMS) radiocarbon dating was done by analysing C_{14} isotopes to estimate the age of the artefacts.

Results and discussion

Visual analysis

On cleaning and sectioning, only sample c was found to have an intact core part, whereas samples a and b were rusted up to the core.

XRF analysis

XRF analysis was carried out to confirm the elements present in the samples. The core parts of the samples were exposed

to Ag-K α radiation. Iron was found to be the major alloying element present in the samples, while silicon was present along with other minor alloying elements (Figure 6).

OM analysis

After polishing and etching with Nital reagent, the microstructures of the samples were observed under OM (Figure 7 a–c). Due to absence of the core part, sample a did not reveal any microstructure (Figure 7). The pits and microcracks observed might be the result of breaking of the oxide layer or delamination. Sample b showed a layered microstructure with two different types of alternate layers (Figure 7). This microstructure was visible only in a small part of the sample. The remaining part of sample b was corroded and did not reveal any grains on most of the sample surface. Further examination at a higher resolution is required to determine the individual layer composition. The microstructure in sample c was distinctly visible (Figure 7 c). The sample showed a coarse grain microstructure along with several

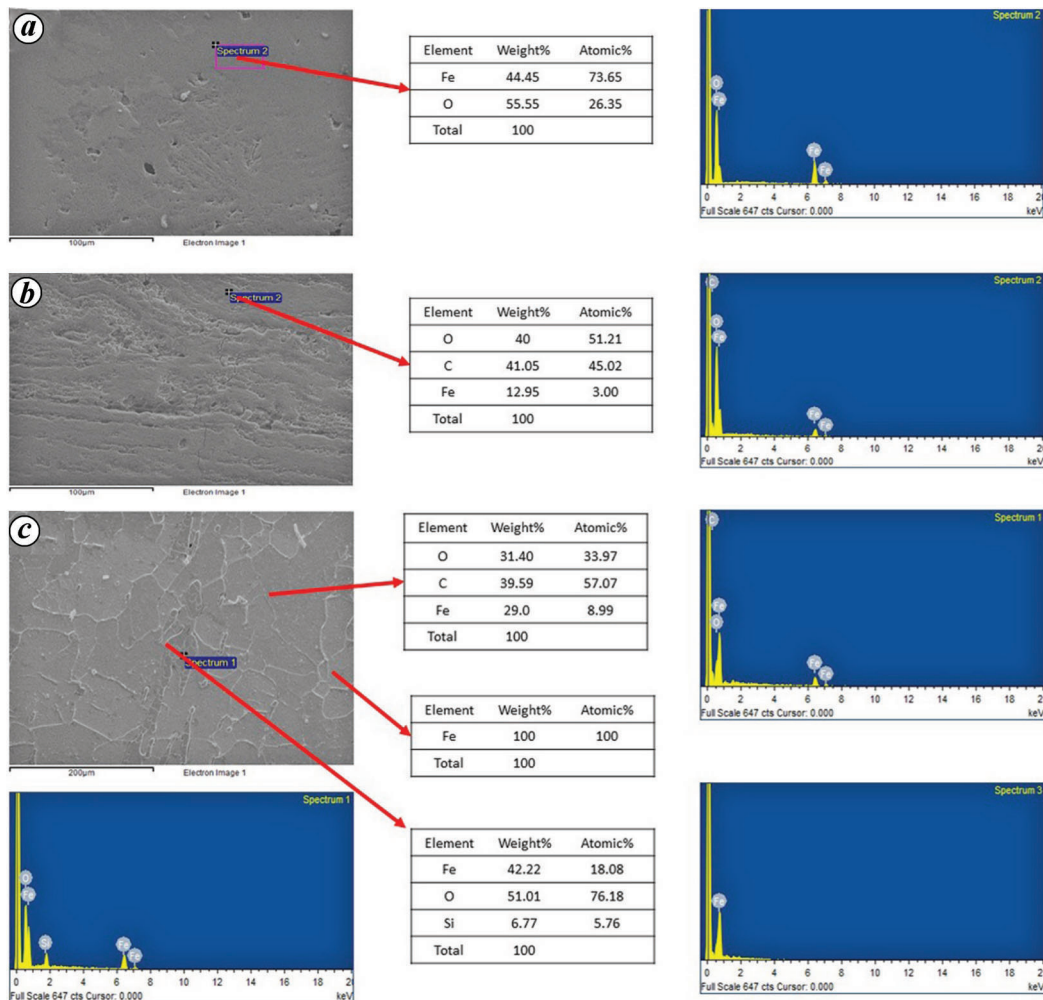


Figure 8. Energy dispersive spectroscopy spectrum and results of (a) sword (sample a), (b) b-sword (sample b) and (c) tripod (sample c).

inclusions. The inclusions were in elongated form, which is a sign of the bloomery iron-making process. In this process, the sponge iron is hammered to make solid steel objects without any holes/porosity¹¹.

SEM analysis

In order to observe the microstructure of the samples with higher resolution, the etched samples were analysed under SEM (Figure 7 d–f). The SEM image of the sample confirmed that almost all surface parts were degraded/corroded and no microstructural features were visible (Figure 7 d). The layered structure of sample b, when observed under SEM revealed that the alternate layers were made of metal and oxides (Figure 7 e). Sample c showed distinct, coarse grain microstructure along with inclusions (Figure 7 f). These inclusions could be a result of the slag entrapment in steel during the bloomery non-making process. In the process, when the iron is smelted on top of the furnace, some slag also entraps in the sponge iron. Though these slag inclu-

sions are removed during post-processing, some inclusions remain in the steel. The microstructure of sample c consisted of pearlite and ferrite grains as the matrix¹².

EDX analysis of samples a and b confirmed that they were corroded to trace any core parts for further analyses (Figure 8 a and b respectively). In contrast, the EDX analysis of sample c confirmed the presence of inclusions in the microstructure. Those belonging to the slag, a compound of Fe, Si, and O (Figure 8 c). EDX analysis of sample c shows the presence of Fe along with C and O. The light grains could be ferrite while the grey grains could be pearlite based on OM and the literature⁶. Thus sample c can be classified as a low-carbon steel object.

Phase identification

XRD of the samples was carried out after mirror polishing to identify the phases present. The cold epoxy-mounted samples were polished. As they were corroded on the surface, the cold epoxy-mounted samples were analysed using XRD,

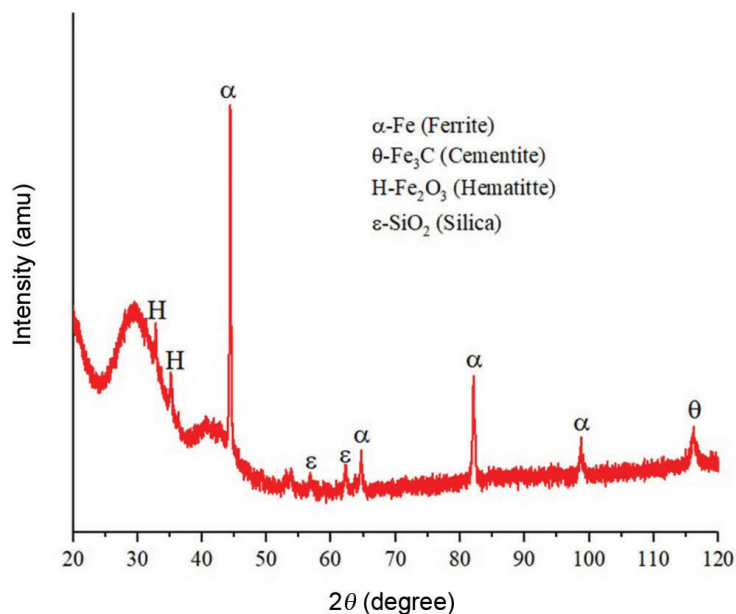


Figure 9. X-ray diffraction spectra of the tripod sample.

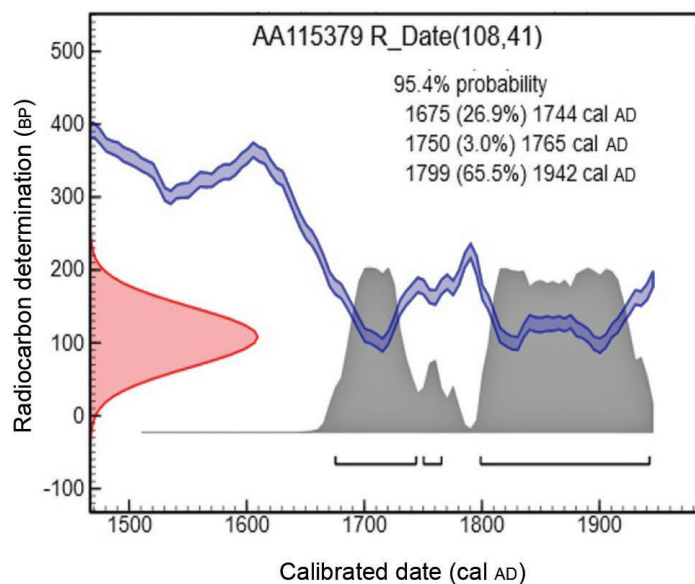


Figure 10. Calibration curve of samples of accelerator mass spectroscopy radiocarbon analysis.

to identify the phases based on crystal structure instead of atomic number of the elements. The sword samples were degraded and no core was present. The sword samples showed noise in the XRD pattern and no conclusions could be made.

XRD pattern of the tripod sample showed a sharp XRD peak along with a hump at a lower Bragg angle (Figure 9). The hump corresponded to epoxy resin. Sharp and distinct peaks were observed corresponding to the crystalline phases. XRD results confirmed the presence of α -Fe and θ -Fe₃C phases in the sample¹³. Corrosion is a degradation process in which a material tries to reach its native state. Due to this,

oxide of iron or hematite (Fe₂O₃) phase was present in the samples¹⁴. The XRD pattern was analysed using 'X'Pert Highscore Plus' software and the SiO₂ (ICSD 98-006-7015) orthorhombic phase was found to be present, which could be a part of the slag constitution. The above analysis confirms that the ferrite and pearlite phases are present in the sample c along with the inclusion.

AMS analysis

AMS radiocarbon analysis was carried out to date the artefacts scientifically. A portion of the sample a was cleaned

by immersion in a weak HCl solution. This process removed accumulated carbonate salts (if any) from the sample surface. When the sample is heated in radiography furnace, the carbon present reacts with the flowing stream of oxygen and forms carbon dioxide. The carbon dioxide was converted to graphite, and the graphite carbon isotope spectrum was measured using AMS. The AMS measurement was calibrated using OxCal v4.4.4 and the most recent 2020 calibration dataset.

The analysis revealed that the half decay time of radioactive carbon was 108 ± 41 years BP. The calibration curve revealed the maximum possible date to be 17th century CE (Figure 10). This is 3000 years younger than the reported age of 1st millennium BCE based on associated finds and morphological features.

Conclusion

Samples of two swords and one tripod from Tripirangode were analysed to understand the iron-making process from the corresponding time. XRF analysis confirmed that the recovered artefacts were iron objects with silicon, aluminium and phosphorus as the minor alloying elements. XRD and EDS analyses were used to identify the phases in the samples. OM and SEM analyses confirmed that the tripod sample contained slag inclusions entrapped during the iron-making process. AMS radiocarbon dating determined the age of the artefacts to be 17th century CE.

This study reveals that samples recovered from the rock-cut cave in Tripirangode are ferrous materials with low-carbon steel. The presence of slag inclusion in the tripod and its low carbon content indicate the smelting method is in the bloomery iron-making process. This process was in use until the 18th century to produce warfare artefacts. The microstructure of the tripod sample contained ferrite and pearlite. The 17th century iron with 1st millennium BCE pottery could be the result of reuse of earlier caves for storing or hiding medieval weapons. This signifies the importance of dating the artefact(s) with absolute dating method like AMS, then relying on the accepted dates of associated finds like that of pottery.

1. Jaikishan, S., Survey of iron and wootz steel production sites in northern Telangana. *Indian J. Hist. Sci.*, 2007, **42**, 445–460.
2. Singh, A. K., Kanungo, A. K., Selvakumar, V. and Arora, A., Ancient high carbon steel from South Tamil Nadu, India: microstructural and elemental analysis, *Curr. Sci.*, 2021, **121**, 239–247.
3. Srinivasan, S., Indian iron and steel, with special reference to southern India. In *The World of Iron*, Archetype Press, London, 2013, pp. 83–90.
4. Thiele, A., Smelting experiments in the early medieval fajszi-type bloomery and the metallurgy of iron bloom, *Period. Polytech. Mech. Eng.*, 2010, **54**, 99–104.
5. Balasubramaniam, R., Pandey, A. and Jaikishan, S., Analysis of wootz steel crucible from northern Telangana. *Indian J. Hist. Sci.*, 2007, **42**, 649–671.
6. Prakash, B., Ancient Indian iron and steel: an archaeometallurgical study. *Indian J. Hist. Sci.*, 2011, **46**, 381–410.
7. Govind, B., Remnants of Iron Age found at Tripirangode: pottery and swords recovered from rock-cut chamber said to be over 2000 years old. *The Hindu* (Kerala edn), 29 August 2020.
8. Melpathur, S., Megalithic age rock-cut chamber and iron weapons discovered from Thirunavaya. *Mathrubhumi Daily* (Malappuram edn), 24 August 2020.
9. <http://d-maps.com> (accessed on 26 December 2021).
10. Rajan, K. and Yatheeskumar, V. P., New evidences on scientific dates for Brāhmī script as revealed from Porunthal and Kodumal excavations, *Prāgdhārā*, 2013, **21–22**, 279–295.
11. Srinivasan, S., Ranganathan, S. and Giunlia-Mair, A., Metals and civilizations. National Institute of Advanced Studies, Bengaluru, 2015.
12. Roy, O. and Krishnan, K., Understanding ancient iron technology of the Vidarbha Megalithic: an archaeo-metallurgical and ethnographic perspective. *Pratna Samiksha*, 2018, **9**, 115–136.
13. Jia, N., Shen, Y. F., Liang, J. W., Feng, X. W., Wang, H. B. and Misra R. D. K., Nanoscale spheroidized cementite induced ultra-high strength–ductility combination in innovatively processed ultrafine-grained low alloy medium-carbon steel. *Sci. Rep.*, 2017, **7**, 2679.
14. Grevey, A. L., Vignal, V., Krawiec, H., Ozga, P., Peche-Quilichini, K., Rivalan, A. and Mazière, F., Microstructure and long-term corrosion of archaeological iron alloy artefacts. *Herit. Sci.*, 2020, **8**, 1–19.

ACKNOWLEDGEMENT. We thank the Ministry of Mines (project number Met4-14/6/2022), for financial support. We also thank the Central Instrumentation Facility of Indian Institute of Technology Gandhinagar for facilitating the use of the FESEM and XRD.

Received 31 May 2022; revised accepted 18 October 2022

doi: 10.18520/cs/v124/i3/333-339